The role of reactive oxygen species on *Plasmodium* melanotic encapsulation in *Anopheles gambiae*

Sanjeev Kumar*†, George K. Christophides†‡, Rafael Cantera§, Bradley Charles*, Yeon Soo Han*¶, Stephan Meister‡, George Dimopoulos‡‖, Fotis C. Kafatos‡, and Carolina Barillas-Mury*,††**

*Colorado State University, Department of Microbiology, Immunology, and Pathology, 1619 Campus Delivery, Fort Collins, CO 80523; ‡European Molecular Biology Laboratory, Meyerhofstrasse 1, 69117 Heidelberg, Germany; and §Zoology Department, Stockholm University, S-10691 Stockholm, Sweden

Contributed by Fotis C. Kafatos, September 29, 2003

Malaria transmission depends on the competence of some *Anopheles* mosquitoes to sustain *Plasmodium* development (susceptibility). A genetically selected refractory strain of *Anopheles gambiae* blocks *Plasmodium* development, melanizing, and encapsulating the parasite in a reaction that begins with tyrosine oxidation, and involves three quantitative trait loci. Morphological and microarray mRNA expression analysis suggest that the refractory and susceptible strains have broad physiological differences, which are related to the production and detoxification of reactive oxygen species. Physiological studies corroborate that the refractory strain is in a chronic state of oxidative stress, which is exacerbated by blood feeding, resulting in increased steady-state levels of reactive oxygen species, which favor melanization of parasites as well as Sephadex beads.

The natural transmission cycle of the malaria parasite, *Plasmodium*, requires completion of a complex developmental cycle in the midgut and salivary glands of the *Anopheles* mosquito vector (1). However, after its entry with the blood meal, the parasite encounters the innate immune responses of the mosquito, which are often robust and coincide with major parasite losses (2–4). At the extreme, the vector is refractory and completely blocks transmission of the parasite. Genetically selected susceptible and refractory strains (4A r/r and L3–5; henceforth S and R, respectively) have been described in the African mosquito, *Anopheles gambiae*. The R strain blocks parasite development in the midgut, oxidatively converting tyrosine to melanin, which crosslinks proteins into a capsule assembled around the parasite (5, 6). Melanotic encapsulation largely depends on three quantitative trait mosquito loci; the *Plasmodium* encapsulation genes *Pen1*, *Pen2*, and *Pen3* that have been mapped (7), although not yet identified with particular sequences. The major locus, *Pen1*, has also been associated with the ability of the R strain to melanize CM-Sephadex beads (8).

When the malaria ookinete passes the refractory mosquito midgut, the melanotic capsule first appears, and is significantly thicker, on the ookinete's apical end facing the hemolymph (6). This observation indicates that key components of the melanization reaction derive from the hemolymph. In a histological and ultrastructural survey of the R and S strains, we noted pronounced differences in their pericardial cells. These are scavenging nephrocytes, which are present alongside the dorsal vessel and that harbor numerous peroxisomes, catalase-rich organelles that are active in detoxification and neutralization of reactive oxygen species (ROS). The pericardial cells of S mosquitoes contain numerous peroxisomes, including some very large ones (Fig. 1*A*), whereas the cells of the R strain possess significantly fewer and smaller peroxisomes (Fig. 1*B*). These morphological differences suggested that the refractory phenotype may result from a systemic deficiency in ROS detoxification.

We have previously used cDNA microarrays to explore the immune and oxidative stress responses in *A. gambiae* cell lines, and the responses to sterile and septic injury as well as malaria infection in adult female mosquitoes (9). Hydrogen peroxide challenge of an immune-competent cell line revealed transcriptomic responses to oxidative stress, including a massive up-regulation of genes implicated in mitochondrial energy metabolism and a free radical defense system. This oxidative stress response did not involve genes implicated in the mosquito's innate immune system, with few exceptions. Challenge of the cells with some microbial components, peptidoglycan, but not lipopolysaccharide, resulted in up-regulation of oxidative stress responsive genes clusters, possibly indicating elicitation of oxidative burst. Preliminary experiments (data not shown) also

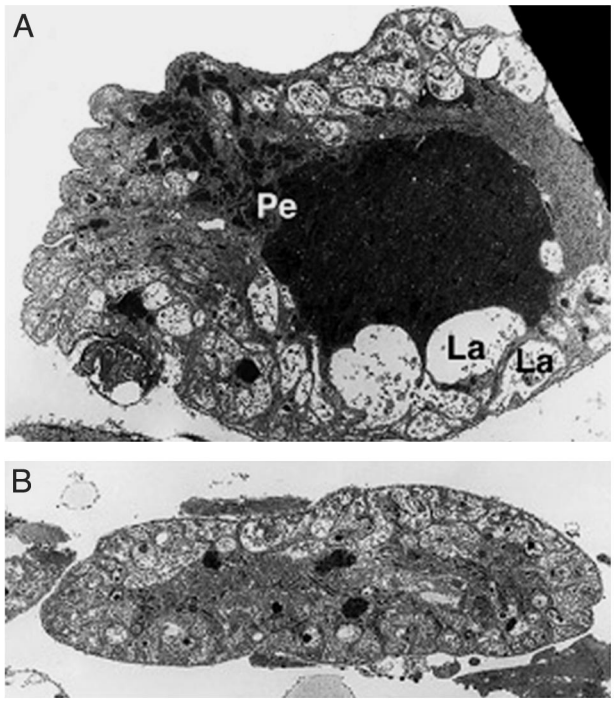

Fig. 1. Electron microscopy images of susceptible (*A*) and refractory (*B*) mosquito pericardial cells. The susceptible mosquito pericardial cells contain a large lacunar space (La), numerous small and large peroxisomes (Pe), and membrane invaginations as in other insects. In the refractory strain (*B*), the pericardial cells are hypotrophic and contain fewer and smaller peroxisomes.

Abbreviations: ROS, reactive oxygen species; SOD, superoxide dismutase; PO, phenoloxidase.

†S.K. and G.K.C. contributed equally to this work.

¶Present address: College of Agriculture and Life Science, Chonnam National University, 300 Yongbong-Dong, Puk-Gu, Gwangju, 500-757, Korea.

‖Present address: Department of Molecular Microbiology and Immunology, The Johns Hopkins University, 615 North Wolfe Street, Baltimore, MD 21205.

**Present address: Laboratory of Malaria and Vector Research, National Institutes of Health, 4 Center Drive, Bethesda, MD 20892.

††To whom correspondence should be addressed. E-mail: cbarillas@niaid.nih.gov.

revealed a number of differences in the expression profiles between naïve S and R female adult mosquitoes that were consistent with the electron microscopy study in suggesting that R mosquitoes have compromised redox metabolism. Here, we report more detailed studies that point to ROS detoxification as a potentially key physiological difference between susceptible and melanotically encapsulating refractory strains. In these studies we used R and S, as well as G3 mosquitoes. The G3 strain is largely susceptible, but not closely related by ancestry, to the S strain. In contrast, the R strain was initially selected from a G3 mosquito colony. Therefore, inclusion of G3 served to control for R vs. S gene expression differences that might arise from polymorphisms unrelated to the refractory trait. The G3 pericardial cells are intermediate in morphology between these of R and S mosquitoes (data not shown).

Methods

A. gambiae Strains. The R and S strains are those previously used to map the refractory trait (7). The R strain, now called L3–5, was derived from the original melanotic strain (5), but the original susceptible strain was lost, necessitating the selection of another S strain, 4A r/r. Like all currently available mosquito strains, the R and S strains have residual polymorphisms. The *A. gambiae* adult female mosquitoes were maintained and blood-fed or infected with *Plasmodium berghei* as described (3, 4).

Microarray Analysis. DNA microarray construction, hybridization, and data analysis were performed as reported (9, 10). Genes showing significant similarity to protein sequence database entries were classified in the most represented functional classes by manual database searches. A combination of K-mean and hierarchical clustering methods was used to assemble differentially expressed sequences into expression clusters that can be correlated with functions.

Electron Microscopy. Female R and S mosquitoes were dissected in PBS and fixed for transmission electron microscopy. The midgut and dorsal half of the abdominal wall with attached epidermis, muscles, tracheae, fat body, heart, and pericardial cells were fixed and processed for transmission electron microscopy as described (11). Toluidine-blue stained 1-μm sections were serially cut from three abdominal segments for each individual and analyzed by light microscopy.

Quantitation of ROS in Hemolymph. The hemocoel of individual females was flushed by injection of 5 μl of PBS containing 2 mg/ml 3-amino triazole (catalase inhibitor), and the hemolymph samples from five mosquitoes were pooled for each measurement. The level of hydrogen peroxide was determined as described (12). Briefly, the samples were incubated at 37°C for 15 min with a mixture containing 250 μM ferrous ammonium sulfate (Mohr's salt), 25 mM H_2SO_4, 100 mM sorbitol, and 50 μM xylenol orange. The change in absorbance of xylenol orange at 550 nm was determined. To estimate superoxide anion levels, the hemolymph sample was incubated with superoxide dismutase (SOD) for 10 min at room temperature to convert superoxide anion to hydrogen peroxide, and the increase in hydrogen peroxide relative to the untreated sample was calculated.

Melanization of Sephadex beads in the L3–5 _A. gambiae_ Strain. CM-Sephadex C25 beads (40–125 μm in diameter) were suspended in sterile mosquito saline (1.3 mM NaCl, 0.5 mM KCl, 0.2 mM $CaCl_2$ and 0.001% methyl green) and one bead was injected into the thorax of each 3-day-old sugar or ascorbic acid-fed female as described (13). Injected mosquitoes were placed in 100% humidity at 28°C for 24 h. The beads were recovered by dissection, were mounted, and their degree of melanization scored into four categories (no melanization, <50%, >50%, and complete melanization). Uric acid (1 mg/ml) was fed to mosquitoes in 10% sugar solution for 2 days before implanting the Sephadex bead.

Phenoloxidase (PO) Activity in the Hemolymph of _A. gambiae_ G3 Mosquitoes. PO activity was measured as described (14, 15). In brief, hemolymph from 75 mosquitoes (2–3 days old) was obtained by flushing the hemocoel with 5 μl of 200 mM Tris·HCl (pH 7.2), individual samples were pooled together and kept on ice. For each reaction, 15 μl of hemolymph were incubated at 28°C in 200 mM Tris·HCl (pH 7.2) with 2 mg/ml dopamine in a 50-μl reaction volume, in the presence or absence of various concentrations of uric acid, vitamin C, or reduced glutathione. After incubation for 15 min, the colored end product of dopamine oxidation was read at 450 nm. The effect of each reagent on PO activity is expressed as the percentage of the activity of a reference sample with no inhibitor.

PCR-Based Cloning of SOD and Catalase. Two well conserved regions were chosen to synthesize degenerate oligonucleotides for superoxide dismutase (5′-CAYGGITTYCAYGTICAYGARTTYGG-3′ and 5′-YTCRTGRTCICCYTGICCIARRTCRTC-3′) and catalase (5′-TTYGGITAYTTYGARGTIACICAYGAYAT-3′ and 5′-GGRCARTTIACIGGDATITGIARRTARTT-3′). A 5′ extension (GCCG**CTCGAG**), which introduces an *Xho*I site (bold), was included in all primers. PCRs were performed by using 20 pmol of each primer, 50 ng of *A. gambiae* G3 genomic DNA template in 50-μl reactions, and AmpliTaq (Perkin–Elmer) with standard buffer conditions (1.5 mM $MgCl_2$). Two initial cycles (1-min steps at 95, 55, and 72°C and 95, 42, and 72°C) were followed by 30 cycles at moderate stringency (1-min steps at 95, 52, and 72°C) and a final 7-min extension at 72°C. The PCR products were cloned (TA cloning kit, Invitrogen), sequenced, and used to design perfect matching primers used for RT-PCR. SOD and catalase were subsequently identified as ENSANGP00000016164 and ENSANGP00000021298 Ensembl predictions, respectively.

RT-PCR. Poly(A) mRNA was isolated from groups of 30 mosquitoes by using Oligotex-dT beads (Qiagen). First-strand cDNA was synthesized by using random hexamers and Superscript II (GIBCO/BRL) for 1 h at 37°C. For expression studies, PCRs were performed by using 20 pmol of each primer in 50-μl reactions and AmpliTaq (Perkin–Elmer) with standard buffer conditions (1.5 mM $MgCl_2$). The primers for SOD were 5′-TGCCGCTAAGGTCAGAAGCAGT-3′ and 5′-TGCGTAGCGGTCAAGTCT-3′ (362 base pairs); and, for catalase, 5′-GCAACAATACGCCCATCTTCTTCA-3′ and 5′-GGAATGAGCGGGAATTCGTT-3′ (496 base pairs). RT-PCR of ribosomal protein gene S7 (16) using standard primers 5′-GGCGATCATCATCTACGTGC-3′ and 5′-GTAGCTGCTGCAAACTTCGG-3′ (461 base pairs) provided the internal control for the amount of cDNA template used. The PCR products were analyzed by agarose gel electrophoresis and the intensity of the bands was determined.

Results

Expression Profiling of Refractory and Susceptible Mosquitoes. We used cDNA microarrays (9) to assess differences in gene expression patterns between R, S, and G3 mosquitoes at 3, 24, and 36 h after blood feeding on mice that were either uninfected or infected with *P. berghei*. The data were first normalized by using sugar-fed mosquitoes of the same strain as reference, and then were subtracted from each other to reveal strain differences. Analysis of all spotted genes indicated that redox-related genes and some putative immunity genes accounted for many of the differences between strains (data not shown). Therefore, we

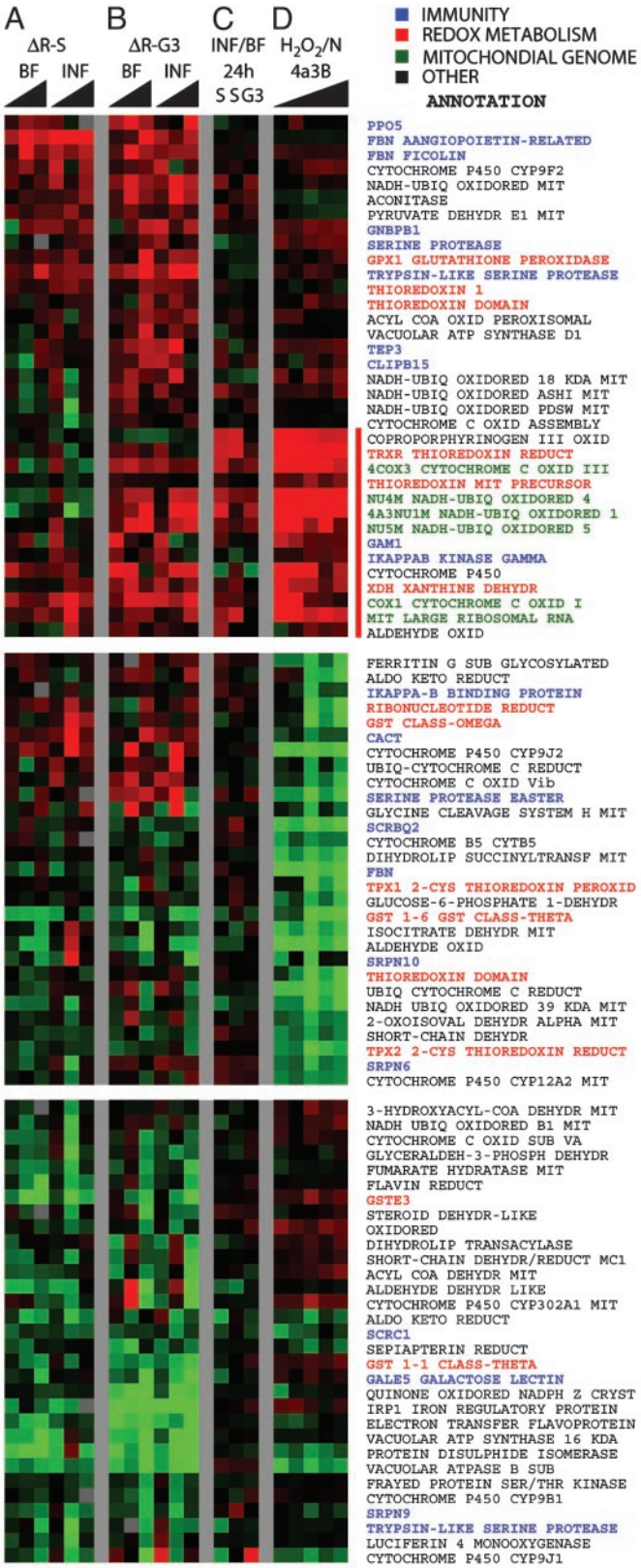

Fig. 2. Transcriptional profiling analyses in R, S, and G3 mosquitoes, including genes involved in immune reactions (blue), redox metabolism, and detoxification (red), genes encoded by the mitochondrial genome (green), and others (black) functioning in the mitochondria or are involved in other oxidoreductive processes. (*A* and *B*) Differences in gene expression between R and S (A, ΔR-S) and R and G3 (B, ΔR-G3) female mosquitoes after blood feeding on healthy mice (BF) or mice infected with *P. berghei* (INF). Gene expression was assessed at 3, 24, and 36 h after blood feeding by using sugar-fed mosquitoes as reference. (*C*) Direct comparison of gene expression in infected and blood-fed-susceptible (S, G3) mosquitoes. (*D*) Expression profiling of *A. gambiae* cells treated with H_2O_2 (9) and assayed 1, 4, 12, 18, and 24 h after challenge. Naïve cells were used as reference. Full annotation of the presented genes can be found in Table 1, which is published as supporting information on the PNAS web site.

extracted and reclustered the data from genes of these two categories, and obtained the strain-subtracted differential profiles shown in Fig. 2 *A* and *B*. We also obtained differential profiles based on the ratio of nonnormalized data from mosquitoes fed on infected vs. noninfected mice (Fig. 2*C*). For comparison, previously reported differential profiles between H_2O_2-treated and nontreated mosquito cell cultures were included (ref. 9 and Fig. 2*D*).

Substantial up-regulation and down-regulation differences were detected on certain genes between the refractory (R) and either of the strains (both ΔR-S and ΔR-G3: Fig. 2 *A* and *B*, respectively); the S and G3 susceptible strains were very similar although not identical in this respect. These differences included many redox-related and some immunity genes. They were mostly due to blood feeding, as they were broadly similar in two parallel time course experiments by using blood-fed uninfected (BF) or infected (INF) mosquitoes of the same strain (Fig. 2 *A* and *B*). This finding is consistent with the known metabolic burst and oxidative stress caused by the blood meal (17). However, when INF and BF mosquitoes of the same strain were compared directly, without prior normalization to sugar-fed mosquitoes, a group of genes that were up-regulated 24 h after infection is highlighted (Fig. 2*C*). Remarkably, these genes were strongly up-regulated by H_2O_2 treatment of cells (Fig. 2*D*); many of them were also more strongly induced in R than in susceptible (especially G3) mosquitoes (Fig. 2 *A* and *B*).

The highlighted group is strongly enriched in genes of the mitochondrial genome. They include genes encoding subunits of the NADH dehydrogenase and cytochrome *c* oxidase complexes of the mitochondria respiratory chain. Nuclear genes encoding subunits of these two complexes are also included. Surprisingly, the gene encoding the large mitochondrial ribosomal RNA is also present in the same expression group; it is represented in the microarray with several EST clones, all of which showed a very consistent induction profile. These expression features may suggest mitochondrial malfunction leading to increased generation of ROS, possibly of superoxide anion. In turn, enhanced ROS levels could cause severe mitochondrial damage that would release apoptosis-inducing factors such as cytochrome *c*. An increasing body of evidence connects apoptosis with parasite invasion of the mosquito midgut (18, 19) (A. Danielli and D. Vlachou, unpublished work).

Three key nuclear-encoded components regulating redox metabolism, namely thioredoxin reductase (TRXR), mitochondrial thioredoxin, and xanthine dehydrogenase (XDH), are also included in this cluster. TRXR is the central enzyme for redox homeostasis in both *Anopheles* and *Drosophila* where glutathione reductase is absent (20, 21). XDH is the key enzyme for production of uric acid, a final product of purine biosynthesis, which also serves as antioxidant and protects bloodsucking insects against hemin-induced oxidative stress (17). However, the production of uric acid by XDH is also coupled with the production of H_2O_2, leading to a local increase of ROS. The free radicals resulting from the combined activity of XDH and other NAD(P)H oxidases, together with nitric oxide synthase, which is up-regulated by parasite infection (4, 18, 22, 23), could lead to locally elevated levels of peroxynitrite and other reactive nitrogen intermediates, mediating oxidative damage of a wide range of biological molecules (24). Additional genes encoding proteins

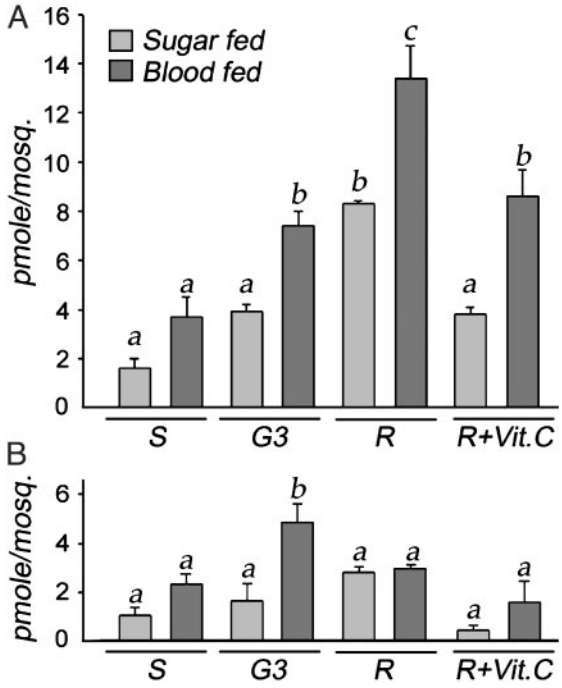

Fig. 3. Levels of ROS in hemolymph of sugar-fed (light shaded bars) or blood-fed (dark shaded bars)-susceptible (S), G3 and refractory (R) females. (*A*) Hydrogen peroxide levels. (*B*) Superoxide anion levels. Vitamin C was administered in larval and adult stages at a dose of 2.5 mg/liter and 25 mg/ml in 10% sucrose for 48 h, respectively. In a given graph, values that are significantly different from each other are labeled with a different letter.

involved in metabolic pathways that take place in the mitochondria (e.g., the Krebs cycle and associated reactions) are also differentially regulated between the R and S or G3 mosquitoes, their biochemical implications remain to be evaluated in more extensive followup studies.

Fig. 2 shows that a number of putative immunity genes are differentially regulated. In particular, genes coding two fibrinogen lectins, two trypsin-like serine proteases (one of them possessing a CLIP domain), the Gram-negative binding protein-1, a prophenoloxidase (PPO5), a thioester containing protein (TEP3), and IκB kinase γ are up-regulated in R mosquitoes after feeding on infected or naïve blood. In *Drosophila melanogaster*, the pattern recognition receptor peptidoglycan-recognition protein and the Toll signaling pathway have recently been shown to participate in the regulation of melanization reactions (25, 26). The elevated expression of several immune genes in the R strain may reflect increased activity of particular immune signaling pathways. In combination, higher activity of some immunity genes and an abnormal redox state of the R, as compared with S or G3 mosquitoes, may contribute significantly to the malaria transmission block and parasite melanization in these mosquitoes.

ROS and Melanization. The differences in morphology and gene expression between the strains led us to propose and test the hypothesis that the R strain is in a chronic state of oxidative stress, and that this physiological state favors the melanotic encapsulation of *Plasmodium*. We determined the level of hydrogen peroxide and superoxide anion in the hemolymph of sugar-fed females from the R, G3, and S strains (Fig. 3, light shaded bars). The R strain had significantly higher basal levels of hydrogen peroxide (Fig. 3*A*) than the two susceptible strains ($P < 0.01$ by ANOVA analysis with the SNK method), whereas the superoxide anion levels (Fig. 3*B*) did not differ. The physiological correlates of the oxidative stress resulting from the increased metabolic activity induced by blood feeding were evaluated by measuring ROS in hemolymph 24 h after a blood meal (Fig. 3, dark shaded bars). An increase in hydrogen peroxide level (Fig. 3*A*) was observed in all strains after blood feeding; the induced level was again higher in the R mosquitoes, and was significantly higher than in the G3 or S strains ($P < 0.01$). The superoxide anion level (Fig. 3*B*) increased significantly after feeding only in the G3 strain, where it reached higher levels than in the R or S strains ($P = 0.016$). Taken together, these data support the hypothesis that the R strain is under a chronic state of oxidative stress, which is exacerbated by the additional physiological stress induced by blood feeding.

We tested the hypothesis that increased levels of ROS in the hemolymph favor the melanotic encapsulation phenotype by administering vitamin C, a strong antioxidant, to R females. As expected, this treatment resulted in a significant decrease in hydrogen peroxide (Fig. 3*A*) in both sugar- and blood-fed females ($P < 0.01$), to levels not significantly different from those of the G3 strain. Vitamin C treatment also seemed to decrease the levels of superoxide anion, albeit not to a significant extent (Fig. 3*B*). The effect of vitamin C treatment on the melanotic encapsulation capacity of the R strain was then evaluated, first by using the CM-Sephadex C25 bead assay; this phenotype has been mapped to the same major QTL (*Pen1*) as parasite encapsulation (8, 13, 27). As shown in Fig. 4*A*, feeding vitamin C to R mosquitoes significantly reduced the melanization of implanted Sephadex beads ($P < 0.001$ by the χ^2 test). Importantly, vitamin C treatment also dramatically reduced the number of encapsulated parasites/midgut, as assayed 36 h after infection: from 31.6 parasites/midgut in control females to 4.8 in vitamin C-treated females fed on the same malaria-infected mouse (Fig. 4*B*). The clear effect of vitamin C could be due to the observed reduction in H_2O_2, or to the direct inhibition of PO enzymatic activity, as reported for *Aedes aegypti* larval extracts (15), or to both factors. We investigated whether vitamin C directly inhibits the PO from *An. gambiae* hemolymph, and we indeed observed an inhibitory effect on PO at concentrations ranging from 0.1 to 1.0 mg/ml (Fig. 4*C*); we suspect that the inhibitory effect of vitamin C on encapsulation is probably due to a combined effect on both ROS and directly on PO activity. To dissect these effects, we tested uric acid, also a strong antioxidant; it was found to have no inhibitory effect on PO *per se* (Fig. 4*C*). Nevertheless, uric acid substantially inhibits melanization in the bead assay (Fig. 4D, $P < 0.001$ by the χ^2 test), indicating that a decrease in ROS by itself can inhibit this process.

Differential Induction of SOD and Catalase mRNAs in Response to Blood Feeding. The analysis of ROS levels in hemolymph suggests that a rate-limiting step in free radical detoxification in the R strain is the clearance of hydrogen peroxide. Given the central role of Cu/Zn SOD and catalase in ROS detoxification, partial cDNAs for these two genes were cloned by using a degenerate primer PCR-based approach. Accumulation of ROS could be the result of decreased production and/or reduced detoxification capacity of these enzymes. Perfect matching primers were designed and used for semiquantitative RT-PCR analysis. Previous experiments in the G3 strain indicated that the midgut is the main organ inducing expression of these two genes during the first 24 h after a blood meal (data not shown). Comparison of the kinetics of midgut mRNA induction (expressed as fold induction relative to sugar-fed time-zero levels) of SOD and catalase revealed striking differences between the strains. SOD mRNA is present at slightly higher levels in sugar-fed S as compared with G3 or R mosquitoes; however, its induction 12 h postfeeding was substantially higher in R (3.65-fold) than in G3 (1.94-fold) or S (0.95-fold) mosquitoes (Fig. 5*A*). Furthermore, this high induc-

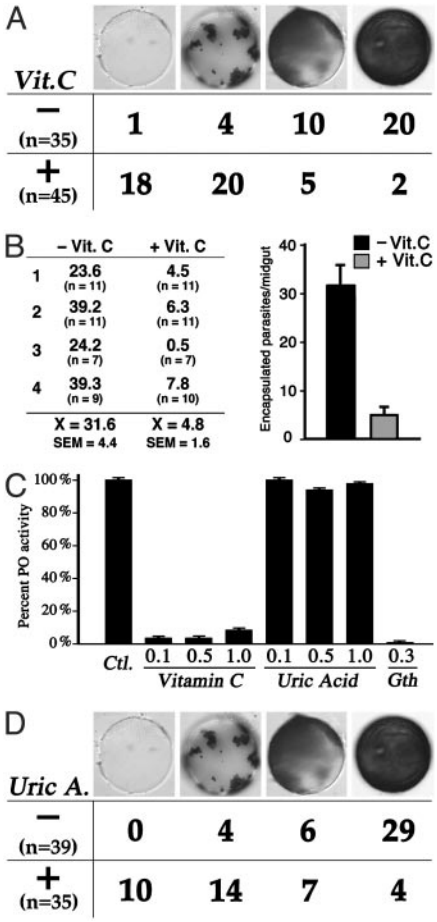

Fig. 4. Suppression of melanization by antioxidants. (*A*) Individual CM-Sephadex (C-25) beads were implanted in 3-day-old R mosquitoes fed with (+) or without (−) vitamin C supplementation during larval stages (2.5 mg/liter) and for 48 h in adult (25 mg/ml in 10% sucrose). The beads were removed 24 h after implantation and scored into four categories, according to the intensity of melanization (no melanization, <50%, >50%, and complete melanization). (*B*) Adult females were supplemented with vitamin C, as described above, and infected with malaria 4–5 days postemergence. The number of parasites encapsulated by control and vitamin C-treated females fed on the same mouse was determined in four independent experiments. (*C*) Effect of different doses of vitamin C and uric acid (mg/ml) on hemolymph PO activity. Glutathione (0.3 mg/ml) results in complete inhibition. The effect of each reagent on PO activity is expressed as the percentage of the activity of reference sample with no inhibitor. (*D*) Same as *A*, but feeding the mosquitoes with uric acid (1 mg/ml) in 10% sucrose.

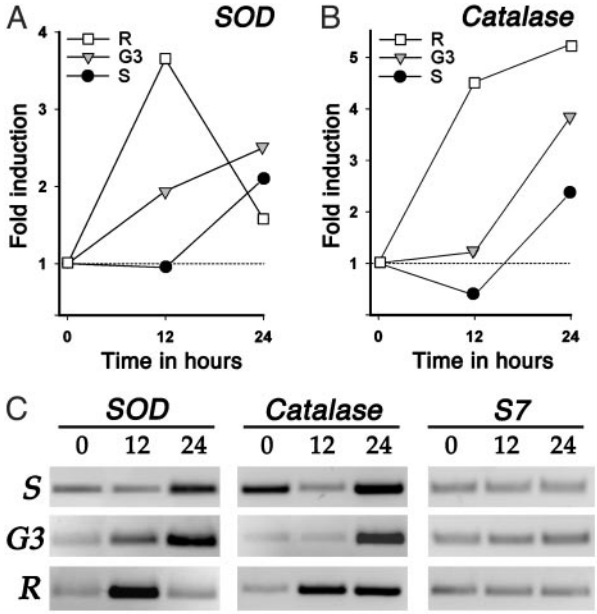

Fig. 5. RT-PCR analysis of midgut mRNA induction in response to bloodfeeding. (*A*) Fold induction of SOD relative to unfed values. (*B*) Fold induction of catalase relative to unfed values. (*C*) Inverted image of the RT-PCR products stained with ethidium bromide after agarose electrophoresis. The intensity of the RT-PCR bands was determined and used to calculate the fold inductions. S7 was used as an internal control to equalize the amount of cDNA template used in all PCRs.

tion was transient, as, by 24 h, the level the mRNA and its induction (1.58-fold) in the R strain was lower than in the G3 (2.5-fold) or S (2.1-fold) strains. Taken together, the data suggest that, after blood feeding, superoxide anion reaches a critical level earlier in the R than in the G3 and the S strains, and that a high transient induction of SOD efficiently converts superoxide anion into hydrogen peroxide (compare the low levels of superoxide anion in hemolymph at 24 h postfeeding in the R strain; Fig. 3*B*).

In sugar-fed females, the S strain midguts express constitutively higher levels of catalase (Fig. 5*C*), which might explain the low level of hydrogen peroxide in hemolymph found in this strain (Fig. 3*A*). As expected, catalase mRNA is induced by the blood meal earlier (12 h) and to higher levels (4.52-fold) in R as compared with G3 (1.22-fold) and S (0.38-fold) mosquitoes (Fig. 5*B*). This induction differs from that of SOD in that the catalase mRNA level continues to increase at 24 h (5.25-fold). Nevertheless, hydrogen peroxide accumulates in the hemocoel. A complete analysis of catalase sequence and protein levels in the S and R strains would be required to establish whether specific mutations might be affecting the catalytic activity, translation, and/or the subcellular location of this enzyme. Interestingly, the catalase gene maps to Chr 2 (21C) in close proximity (170 kb) from microsatellite AG2H135, which is linked to parasite encapsulation in the *Pen3* QTL region.

Discussion

Analysis of gene expression using microarrays and RT-PCR and morphological studies of detoxification organs/cells clearly point to broad physiological differences between the refractory and susceptible strains, suggesting differences in their oxidative status. Direct measurements of ROS in hemolymph confirm that hydrogen peroxide levels increase in response to blood feeding, and that the R strain reaches significantly higher levels than the S or G3 strains. Dietary treatment of the R strain with vitamin C decreases the level of hydrogen peroxide to a level similar to that in G3, and this result is correlated with decreased bead and parasite encapsulation. Dietary treatment with another antioxidant also substantially decreased bead melanization without affecting the PO enzymatic activity. The premature induction of SOD in the R strain suggests that an excess of superoxide anion is produced, but is readily converted to hydrogen peroxide and does not accumulate in the hemolymph. Catalase mRNA expression is induced early and persistently in the R strain, but the hydrogen peroxide level nevertheless increases, suggesting a detoxification deficiency. Based on its chromosomal location and the physiological differences between strains, catalase is a candidate gene responsible for the enhancement of parasite encapsulation ascribed to the QTL of the *Pen3* region. The ultrastructural differences in peroxisome size and number suggest that mutations affecting the biogenesis of this organelle may contribute to the encapsulation phenotype.

The specific mechanism by which increased levels of ROS lead to parasite encapsulation remains to be established, but one can envision at least two nonmutually exclusive scenarios: (*i*) the ROS may themselves exert irreversible damage to the parasite, which secondarily triggers immune recognition and melanization; and (*ii*) increased levels of ROS may accelerate immune activation and/or melanization. It is also possible that the immune system of the mosquito hemolymph may be able to recognize ookinete, but not oocyst surface proteins, and that survival of the parasite depends on the relative rates of the developmental change in its surface proteins vs. the propensity of different vector strains for immune activation and/or melanization. We have used an integrated morphological, physiological, and postgenomic approach to implicate ROS levels as one factor contributing to the melanotic encapsulation phenotype of the R strain. Complete causal analysis of this phenotype will require further multidisciplinary studies.

We thank Evgeny Zdobnov for his assistance in gene annotation and EST clustering and Claudia Blass for valuable technical assistance in microarray construction. This work was supported by National Institute of Allergy and Infectious Diseases–National Institutes of Health Research Grant R01AI45573, National Institute of Allergy and Infectious Diseases–National Institutes of Health Exploratory/Developmental Research Grant U01 AI48846, National Institute of Allergy and Infectious Diseases–National Institutes of Health Program Project Grant P01 AI44220, and European Commission Research Training Networks Grants HPRN-CT-2000–00080. R.C. was supported by a short-term European Molecular Biology Organization fellowship and G.K.C. was initially supported by a European Commission Marie Curie Fellowship.

1. Ghosh, A., Edwards, M. J. & Jacobs-Lorena, M. (2000) *Parasitol. Today* **16,** 196–201.
2. Hoffmann, J. A., Kafatos, F. C., Janeway, C. A. & Ezekowitz, R. A. (1999) *Science* **284,** 1313–1318.
3. Dimopoulos, G., Richman, A., Muller, H. M. & Kafatos, F. C. (1997) *Proc. Natl. Acad. Sci. USA* **94,** 11508–11513.
4. Dimopoulos, G., Seeley, D., Wolf, A. & Kafatos, F. C. (1998) *EMBO J.* **17,** 6115–6123.
5. Collins, F. H., Sakai, R. K., Vernick, K. D., Paskewitz, S., Seeley, D. C., Miller, L. H., Collins, W. E., Campbell, C. C. & Gwadz, R. W. (1986) *Science* **234,** 607–610.
6. Paskewitz, S. M., Brown, M. R., Lea, A. O. & Collins, F. H. (1988) *J. Parasitol.* **74,** 432–439.
7. Zheng, L., Cornel, A. J., Wang, R., Erfle, H., Voss, H., Ansorge, W., Kafatos, F. C. & Collins, F. H. (1997) *Science* **276,** 425–428.
8. Gorman, M. J., Severson, D. W., Cornel, A. J., Collins, F. H. & Paskewitz, S. M. (1997) *Genetics* **146,** 965–971.
9. Dimopoulos, G., Christophides, G. K., Meister, S., Schultz, J., White, K. P., Barillas-Mury, C. & Kafatos, F. C. (2002) *Proc. Natl. Acad. Sci. USA* **99,** 8814–8819.
10. Dimopoulos, G., Casavant, T. L., Chang, S., Scheetz, T., Roberts, C., Donohue, M., Schultz, J., Benes, V., Bork, P., Ansorge, W., *et al.* (2000) *Proc. Natl. Acad. Sci. USA* **97,** 6619–6624.
11. Cantera, R. & Trujillo-Cenoz, O. (1996) *Microsc. Res. Tech.* **35,** 285–293.
12. Jiang, Z. Y., Hunt, J. V. & Wolff, S. P. (1992) *Anal. Biochem.* **202,** 384–389.
13. Gorman, M. J., Cornel, A. J., Collins, F. H. & Paskewitz, S. M. (1996) *Exp. Parasitol.* **84,** 380–386.
14. Lanz-Mendoza, H., Hernandez-Martinez, S., Ku-Lopez, M., Rodriguez Mdel, C., Herrera-Ortiz, A. & Rodriguez, M. H. (2002) *J. Parasitol.* **88,** 702–706.
15. Li, J., Zhao, X. & Christensen, B. M. (1994) *Insect Biochem. Mol. Biol.* **24,** 1043–1049.
16. Salazar, C. E., Mills-Hamm, D., Kumar, V. & Collins, F. H. (1993) *Nucleic Acids Res.* **21,** 4147.
17. Souza, A. V., Petretski, J. H., Demasi, M., Bechara, E. J. & Oliveira, P. L. (1997) *Free Radical Biol. Med.* **22,** 209–214.
18. Han, Y. S., Thompson, J., Kafatos, F. C. & Barillas-Mury, C. (2000) *EMBO J.* **19,** 6030–6040.
19. Zieler, H. & Dvorak, J. A. (2000) *Proc. Natl. Acad. Sci. USA* **97,** 11516–11521.
20. Kanzok, S. M., Fechner, A., Bauer, H., Ulschmid, J. K., Muller, H. M., Botella-Munoz, J., Schneuwly, S., Schirmer, R. & Becker, K. (2001) *Science* **291,** 643–646.
21. Zdobnov, E. M., von Mering, C., Letunic, I., Torrents, D., Suyama, M., Copley, R. R., Christophides, G. K., Thomasova, D., Holt, R. A., Subramanian, G. M., *et al.* (2002) *Science* **298,** 149–159.
22. Luckhart, S., Vodovotz, Y., Cui, L. & Rosenberg, R. (1998) *Proc. Natl. Acad. Sci. USA* **95,** 5700–5705.
23. Luckhart, S. & Li, K. (2001) *Insect Biochem. Mol. Biol.* **31,** 249–256.
24. Godber, B. L., Doel, J. J., Durgan, J., Eisenthal, R. & Harrison, R. (2000) *FEBS Lett.* **475,** 93–96.
25. Ligoxygakis, P., Pelte, N., Ji, C., Leclerc, V., Duvic, B., Belvin, M., Jiang, H., Hoffmann, J. A. & Reichhart, J. M. (2002) *EMBO J.* **21,** 6330–6337.
26. Takehana, A., Katsuyama, T., Yano, T., Oshima, Y., Takada, H., Aigaki, T. & Kurata, S. (2002) *Proc. Natl. Acad. Sci. USA* **99,** 13705–13710.
27. Gorman, M. J. & Paskewitz, S. M. (1997) *Am. J. Trop. Med. Hyg.* **56,** 446–451.